RSC Advances

ROYAL SOCIETY OF CHEMISTRY

www.rsc.org/advances

Cite this: DOI: 10.1039/c0xx00000x

www.rsc.org/xxxxxx

ARTICLE TYPE

Nanoscale zeolitic imidazolate framework-8 as a selective adsorbent for theophylline over caffeine and diprophylline†

Zhong-Ying Liu,[a] Jin-Long Chen,*[ab] Xiao-Yan Sun,[c] Meng-Xiang Su,[ab] Bo Li,[ab] Fang Yan[ab] and Bin Di*[ab]

Received (in XXX, XXX) Xth XXXXXXXXX 20XX, Accepted Xth XXXXXXXXX 20XX

DOI: 10.1039/b000000x

In this work, we firstly explored zeolitic imidazolate framework-8 (ZIF-8) as a novel adsorbent for selective adsorption of theophylline (TPE) over its structure-related analogs involving caffeine (CFE) and diprophylline (DPE) in aqueous solution in view of sole and mixed adsorption, desorption, and solid phase extraction. The adsorption kinetics of TPE on ZIF-8 obeyed a pseudo-second-order kinetics. Analysis of the intraparticle diffusion plots revealed that more than one process affected the adsorption, and film (boundary layer) diffusion controlled the adsorption rate at the beginning stage. The adsorption isotherms of TPE on ZIF-8 followed the Freundlich model, and an enthalpy rather than entropy controlled its adsorption. Evidences from FT-IR and X-ray photoelectron spectroscopic data identified that the adsorption of TPE was also driven by coordination of unsaturated zinc species in ZIF-8 with the carbonyl groups in TPE besides π−π interaction and molecular size. All these interactions made the ZIF-8 a promising candidate for the selective adsorption and extraction of structure-related analogs.

Introduction

Theophylline (TPE) is a well-known xanthine skeleton of alkaloid from tea leaves and coffee beans.[1-3]It bears several similar physical and pharmacological properties to its analogs depending upon their molecular structures as shown in Scheme 1. Theophylline shows great bronchodilator and vasodilator effects which is widely used in the treatment of respiratory disorders like asthma, cardiac dyspnea, and bronchitis. It acts as an adenosine receptor antagonist and phosphodiesterase inhibitor, and so on.[4] However, an overdose of theophylline could be toxic and has been occasionally proved fatal. Toxic effects are often characterized by frequent vomiting and unusual thirst, and in severe cases are followed by convulsions, shock, and death. Furthermore, there is a pronounced intersubject variation in its biological half-life and its therapeutic response appears to be related to the corresponding concentration in biofluids.[5] Therefore, the effective separation and reliable quantification of TPE over its derivates are becoming more and more attractive. Unfortunately, xanthine alkaloids with similar configurations cannot be separated and extracted easily by traditional separation and extraction methods. To date, there have been a few methods and techniques reported to quantitative extraction of TPE from its isomeride aqueous solution and plasma sample,[6-11] such as organic solvent (chloroform),[6] syringe-type minicolume of liquid chromatography,[7] capillary electro-chromatography,[8] a series of molecular imprinted based polymer,[9] film[10] and membrane.[11] But their limitations arise from low extraction capacity, long extraction time, high energy-consumption, complex operations, and toxicity of organic solvents, and so on. The adsorption on porous adsorbents is an economical and effective approach for the extraction of TPE from water solution.

The use of a home-made phenolic resin adsorbent of JDW-2 for extraction of caffeine and theophylline gave a considerable saturation sorption capacity of 246 and 127 mg/g on dried resin respectively, much higher than that of commercially available Duolite S-761 respectively.[12]However, the high adsorption capacity was also limited from difficulty to be produced and complex operations. Therefore, exploring new adsorbents for efficient adsorption and extraction of TPE is still of significance and challenge.

Metal-organic frameworks (MOFs) are a class of fascinating porous materials constructed by metal ions or clusters and organic ligands. MOFs have attracted great attention in numerous applications over the last decade due to their highly diversified structures, tunable pore sizes, large surface areas and tailorable functionalities.[13] The unique structures and specific features also make MOFs a class of excellent adsorbents for adsorptive application from small molecules to biological molecules.[14,15] Zeolitic imidazolate Frameworks (ZIFs), a sub-family of MOFs, are porous crystalline materials with open-framework zeolite

[a]*Department of Pharmaceutical Analysis, China Pharmaceutical University, Nanjing 210009, China. Fax: +86 2583271269; Tel: +86 2593271269; Email: dibin@cpu.edu.cn; chenjl_4@hotmail.com*

[b]*Key Laboratory of Drug Quality Control and Pharmacovigilance (China Pharmaceutical University), Ministry of Education, Nanjing 210009, China*

[c]*Laboratory of Cellular and molecular Biology, Jiangsu Province Institute of Chinese Medicine, Nanjing,210000,China*

[1]*Jin-Long Chen and Zhong-Ying Liu contributed equally to this work*

†Electronic supplementary information (ESI) available. See DOI: 10.1039/b000000x

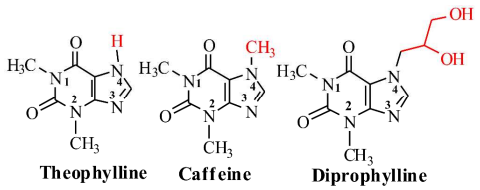

Scheme.1 Molecular structure of theophylline (TPE), caffeine (CFE) and diprophylline (DPE)

structures composed of imidazolate-derived ligands and transition metal ions. Zeolitic imidazolate framework-8 (ZIF-8), a prototypical ZIF material formed by 2-methylimidazole served as a bridging ligand between zinc central ions characterized by sodalite zeolite-type structure containing larger cavities (11.6 Å) and small apertures (3.4Å).[16,17] Besides，it is necessary to note that ZIF-8 was favoured with a striking feature of high chemical and thermal stability in the presence of boiling water, aqueous NaOH, organic solvents and even high pressure.[16,18]The exceptional environment of resistance and unique structure characteristics of ZIF-8 strongly made it a promising candidate for separation and extraction of the analytes in gaseous and aqueous matrix. Furthermore, ZIF-8 could be produced in the powders, thick membranes, thin films and nanocomposites[19] as an amazing absorbent facilitation in realization of micro-/solid-phase extraction,[20-23] molecular sieving of gas separation[24, 25], sensing,[26] pesudostationary phase[27], stationary phase of chromatography[28] and adsorptive removal of dyes,[29] furfural, [30]hazardous materials such as arsenate,[31] benzotriazoles[32]and so on.

However, there have been few reports to utilize the MOFs including ZIF-8 in the selective adsorption and extraction of pharmaceutical molecules especially for drug analogs so far.[20-23, 33]Herein, we take the advantages of structure features and environment of resistance of zeolitic imidazolate framework-8 (ZIF-8) as a novel adsorbent for selective adsorption of TPE over its analogs of caffeine (CFE) and diprophylline (DPE) in aqueous solution, resulted from molecular size based gated effect, π-π interaction, hydrogen bonding and unsaturated Zn-O coordination interaction. The adsorption of TPE on ZIF-8 was studied in view of pH, ionic strength and kinetics in detail. Results for exploration of ZIF-8 for pseudo-solid phase extraction and desorption of TPE, CFE and DPE in aqueous and plasma matrix make ZIF-8 a promising candidate for the selective adsorption and extraction of pharmaceutical analogs in biofluids.

Experimental

Chemicals and materials

All of the chemicals used were at least of analytical grade. 2-Methylimidazole (H-MeIM) and diprophylline were purchased from J&K Scientific Ltd. $Zn(NO)_3 \cdot 6H_2O$ was purchased from Xilong chemical co., Ltd. Theophylline and caffeine were purchased from sigma-aldrich. Methanol (MeOH), acetonitrile and ammonia water were purchased from Nanjing Chemical Reagent Co., Ltd. Ultrapure water （RO-DI water purification through PL5242 Purelab Classic UV (PALL Co. Ltd., USA) to a resistivity of 18.2 MΩ·cm. Plasma was provided by China Pharmaceutical University Hospital. Carton of Yili milk was bought from the local supermarket.

Synthesis of ZIF nanocrystals

ZIF-8 nanocrystals were prepared according to previous article[20]. Typically, a solution containing 2-methylimida-zole (8.3 g) and MeOH (60 mL) was poured into a solution containing Zn $(NO_3)_2 \cdot 6H_2O$ (3.0 g) and MeOH (60 mL), and then the mixture was stirred for 15 min in a water bath (70 ºC). The ZIF-8 nanocrystals were obtained from the milky dispersion by centrifugation at 4000 rpm for 20 min, and then washed with fresh MeOH at three times to remove the unreacted 2-methylimidazole from ZIF-8. Finally, the nanocrystals were dried at 100 ºC in air overnight.

Instrumentation

Transmission electron microscopy (TEM) was performed using a Tecnai G2 20 analyzer (FEI, Norcross, USA) at an accelerating voltage of 120 kV. The nitrogen sorption experiments were performed at -196 °C on ASAP-2020 (Micromertics, Atlanta, GA, USA). The samples were out gassed at 80 ºC for 5 h before the measurement. The Horvath-Kawazoe Differential Pore Volume (HK) method was used to calculate the pore size distribution for the adsorbents. The X-ray diffraction (XRD) patterns were recorded with a D8 advance X-ray diffractometer using Cu K_α radiation over the angular range from 3° to 40° . IR spectra were recorded on a JASCO FT/IR-4100 spectrometer. TGA of ZIF-8 was performed on a Netzsch TG 209 thermal gravimetric analyzer in a continuous-flow nitrogen atmosphere from 30 ℃ to 700 ℃ at a ramp rate of 10 $Kmin^{-1}$.The X-ray photoelecrtron spectroscopy (XPS) measurements were carried out on ESCALAB250 Xi (Thermo, USA) fitted with a monochromated Al Kα X-ray source (hν = 1486.6 eV). UV-vis scans were performed on UV-1700 spectrometer (Shimadzu Corporation, Kyoto, Japan). HPLC separations were performed using a Shimadzu LC-20AT prominence HPLC system (Shimadzu Corporation, Kyoto, Japan).

Effects of pH, and ionic strength

To study the effect of pH, TPE was dissolved in the aqueous solution of 0.01 M NaCl as the control of ionic strength, and the pH was adjusted with Tris and HCl. To evaluate the effects of ionic strength, the TPE solutions were prepared by dissolving TPE in pure water including different concentrations of salt of NaCl.

Adsorption kinetics of TPE on ZIF-8

To study the adsorption kinetics, 5 mL of a fixed initial concentration of TPE solution were added into a 10 mL centrifugal tube containing 10.0 mg ZIF-8 at 25 ℃. After adsorption for a predetermined time (from 15 to 2520 min), the mixture was filtered with 0.22 μm Millipore cellulose membrane, and the filtrate was sampled for HPLC analysis with the injection volume of 20 μL.

Adsorption equilibrium and thermodynamics for the adsorption of TPE on ZIF-8

For a thermodynamic study, the static adsorption proceeded for 72 h to reach adsorption equilibrium at different temperatures (283K, 293K and 303K). For a thermodynamic study, the static adsorption proceeded for 72 h to reach adsorption equilibrium at different temperatures (283K, 293K and 303K). 5 mL of a fixed initial concentration (from 25 to 300 mg L^{-1}) of TPE were added into a 10 mL centrifugal tube containing 10.0 mg ZIF-8. After

adsorption for 72h at three temperatures above-mentioned, respectively, filtered with 0.22 μm Millipore cellulose membranes and the filtrate was sampled for HPLC analysis.

Selective adsorption experiments for TPE over its analogs of CFE and DPE

Solution (5 ml, 100 mg L^{-1}) containing of TPE, DPE and CFE respectively was adsorbed by ZIF-8(10 mg) at room temperature for 2 hours, and then analysized by UV-Vis in full scan. A mixture solution (5ml, 100 mg L^{-1}) containing TPE, DPE and CFE was adsorbed by ZIF-8(30 mg) at room temperature for 2 hours. The filtration was collected for HPLC analysis.

Results and discussion

Characterization of the prepared ZIF-8 nanocrystals

The prepared ZIF-8 was characterized by XRD, TGA, TEM and N_2 adsorption–desorption experiment (Fig. 1). The experimental XRD pattern (Fig.1a) of the synthesized ZIF-8 was agreed well with the simulated one from its single crystal structure, showing the successful preparation of ZIF-8 with pure phase. The TGA data reveals that the ZIF-8 was stable up to 448°C. The average crystallite diameter of as prepared ZIF-8 is 400 nm featuring with a perspective rhombic dodecahedral crystal as shown in the inset of Fig.1d. The N_2 adsorption result display the type I isotherms and exhibited the Langmuir surface area of ZIF-8 2205 m^2 g^{-1} and the volume of pore is 0.89 cm^3 g^{-1}. A bimodal pore size (calcd. by the HK method) distribution centering at 11.6 and 17.0 Å (Fig.1b inset).[16]

Adsorption experiments for TPE over its analogs of CFE and DPE

In this work, we take the advantages of structure features and exceptional chemical stability of ZIF-8 as a robust adsorbent for selective adsorption of TPE over its analogs of caffeine (CFE) and diprophylline (DPE) in aqueous solution. In the preliminary solely adsorptive experimental, a characteristic absorption band centred at 270 nm with a similar absorption profile originating from xanthine moiety was observed for TPE, CFE, and DPE respectively as shown in Fig. 2a, b and c. Only an essential differential absorption was found for the TPE, while slighter absorption changes of CFE than DPE without obvious band-shift before and after adsorption on ZIF-8. Furthermore, a similar performance was found in the mixture solution of TPE, CFE and DPE before and after adsorption on ZIF-8 analysed by HPLC-UV as shown in Fig. 2d. Results for the adsorption experiments described above implied that ZIF-8 possess the promising capability of selective adsorption of pharmaceutical molecule over its analogs only with an alteration of substituent.

Effect of pH and ionic strength on the adsorption of TPE on ZIF-8

The effect of pH on the adsorption of TPE was studied in the pH range from 3 to 11 in the presence of 1.0 mM Tris-HCl buffer solution. The surface charge and stability of ZIF-8 nanocrystals and the ionization degree of TPE (pK_{a1} = 1.6, pK_{a2} = 8.6) are affected by pH of solution. According to the previous reports on zeta potential of ZIF-8, ZIF-8 is positively charged in the pH of range 2-10,[32] and the charge of TPE could be positive at pH< pK_{a1}, zwitterionic in the range of pK_{a1} to pK_{a2}, while negative at pH > pK_{a2}. The adsorption capacity of ZIF-8 for TPE kept scarcely constant at the pH lower than pK_{a2}, while an unexpected

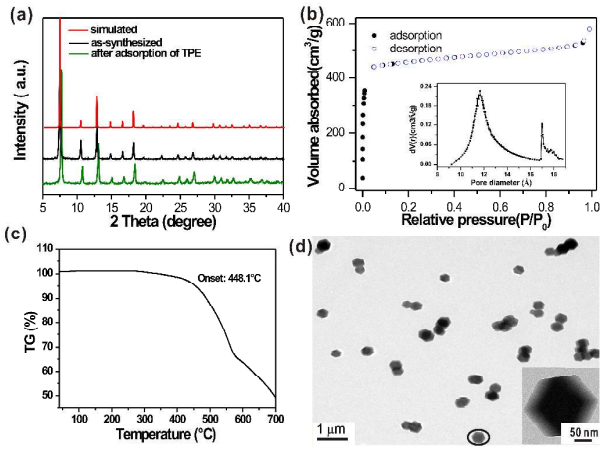

Fig.1 (a) The XRD patterns of the as-synthesized ZIF-8 with the simulated one from its single crystal structure and after adsorption of TPE; (b) Nitrogen-sorption-isotherm and the pore size distribution of the as-synthesized ZIF-8 (inset) (c)TGA curve of the as-synthesized ZIF-8 (d) TEM images of the as-synthesized ZIF-8 nanocrystals (Inset: a representative ZIF-8 nanocrystal).

significant decreasing of adsorption for negative charged TPE molecule with increasing the pH higher than pK_{a2} as shown in Fig. S2. Furthermore, different concentrations of NaCl from 0.01 mol $L^{-1}$to 0.1 mol L^{-1} were used to evaluate the influence of ionic strength on the adsorption of TPE on ZIF-8 (Fig.S3). No obvious loss of the adsorption capacity was observed in different ionic strength. Therefore, electrostatic interaction gave negligible effect on the adsorption capacity of ZIF-8 for TPE.

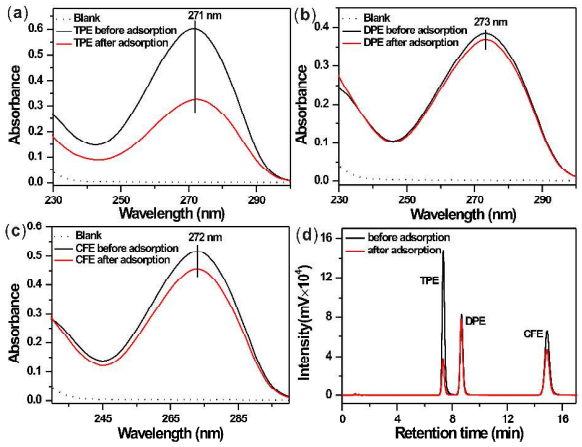

Fig.2 UV-vis spectra for the solutions of 100 mg L^{-1} of TPE (a), DPE (b) and CFE (c) before and after adsorption on 10 mg of ZIF-8 under stirring for 2h at 25 °C, respectively. (d) HPLC-UV chromatogram for the mixture solution of 100 mg L^{-1} TPE, DPE and CFE before and after adsorption on 30 mg ZIF-8 under stirring for 2h at 25 °C.

Adsorption kinetics of TPE on ZIF-8

The time-dependent adsorption of TPE on ZIF-8 was used to study the kinetics for adsorption of TPE on ZIF-8 at five initial concentrations (25, 50, 100, 200, and 300 mg L^{-1}) as shown in Fig. 4. The adsorption capacity significantly increased in the first 8 h and reached equilibrium gradually after 24 h. Moreover, the adsorption capacity significantly increased as the initial concentration of TPE increased, indicating the favourable

adsorption at high concentrations of TPE. However, the unexpected decrease adsorption at low concentration may caused by the more water molecule intrude into the materials. The timely adsorption of TPE on ZIF-8 is well described by a versatile

Table 1 Kinetics parameters for the adsorption of TPE on ZIF-8 at 298 K[a]

		Pseudo-second-order kinetic model			Intraparticle diffusion model		
C_0/mg L^{-1}	$q_{e(exp)}$/mg g-1	$q_{e(cal)}$/mg g^{-1}	k_2/g mg^{-1} min^{-1}	R^2	I	k_{il}/mg g^{-1} $min^{-0.5}$	R^2
25	4.52	4.37	1.77×10^{-1}	0.9824	5.88	1.34	0.9179
50	14.36	11.53	2.51×10^{-1}	0.9581	8.66	3.07	0.9323
100	33.99	34.60	2.68×10^{-2}	0.9969	15.59	2.87	0.9589
200	69.09	76.92	3.64×10^{-3}	0.9770	16.45	3.88	0.8442
300	97.83	107.53	2.64×10^{-3}	0.9835	19.62	8.61	0.7802

[a]Notes: C_0, initial concentration of TPE; $q_{e(cal)}$, calculated adsorption capacity; $q_{e(exp)}$,experimental adsorption capacity; k_2, pesudo-second-order kinetic constant; k_{il}, intraparticle diffusion rate constant for the first linear portion; and I, intercept for the first portion.

pseudo-second-order kinetic model which is based on the adsorption capacity on the solid phase and is in agreement with a chemisorption mechanism being the rate controlling step [34-37](eqn (1)):

$$\frac{t}{q_t} = \frac{1}{k_2 q_e^2} + \frac{t}{q_e} \quad (1)$$

Where q_t and q_e are the adsorption capacity (mg g^{-1}) at a certain time t (min) and equilibrium, respectively, and k_2 is the rate constant for the pseudo-second-order adsorption (g mg^{-1} min^{-1}). The plots of t/q_t against t show good linearity ($R^2 > 0.95$) with a slope of $1/q_e$ and an intercept of $1/(k_2 q_e^2)$. The calculated values of q_e and k_2 are summarized in Table 1. The equilibrium adsorption capacity q_e increased from 12.1 to 146 mg g^{-1} as initial concentration varied from 25 to 300 mg L^{-1}. As the initial concentration increased, the value of k_2 decreased, indicating that chemisorption was significant in the rate-limiting step, involving valency forces through sharing or exchange of electrons between TPE and ZIF-8. The kinetic performance was further analyzed with the intraparticle diffusion model (eqn (2)) to explain if the diffusion mechanism was involved in the adsorption of TPE on ZIF-8. Where q_t (mg g^{-1}) is the adsorption capacity at any time t (min), k_i (mg $g^{-1}min^{0.5}$) the intraparticle diffusion rate constant, and I the intercept. The k_i value can be obtained from the slope of q_t against $t^{0.5}$ plot.

$$q_t = k_i t^{0.5} + I \quad (2)$$

If the value of I is zero, then the rate of adsorption is controlled by intraparticle diffusion for the entire adsorption period.[38] However, the plot of q_t against $t^{0.5}$ shows multilinear portions performance (Fig. S5), suggesting that more than one process gives an effect on the adsorption.[39] The values of the slopes of q_t against $t^{0.5}$ plots are not zero as well implying that film (boundary layer) diffusion controlled the adsorption rate at the beginning stage.[40]

The multiple natures observed in the intraparticle diffusion plots suggest that intraparticle diffusion is not solely rate-limiting step.[41]

Adsorption equilibrium study

Figure S5 shows the adsorption isotherms of TPE on ZIF-8 at 283K, 293K and 303K. These data could be approximated by the Freundlich isotherm model, which depicts the relationship between the amount of TPE adsorbed by per unit mass of ZIF-8 (q_e, mg g^{-1}) and the equilibrium concentration of TPE (C_e, mg L^{-1}) in solution:

$$q_e = K_F C_e^{1/n} \quad (3)$$

Where, K_F and n are the Freundlich constants related to the adsorption capacity and adsorption intensity, respectively.

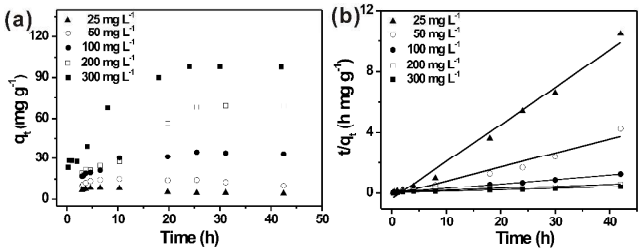

Fig.3 Time-dependent adsorption of TPE (a) and the plots of pseudo-second-order kinetics for the adsorption of TPE (b) at different initial concentrations: (▲) 25, (○) 50, (●) 100, (□) 200, and (■) 300 mg L^{-1} on ZIF-8 at 25 °C and pH 8.0

The Freundlich equation is applicable to highly heterogeneous surfaces, and an adsorption isotherm lacking a plateau indicates a multi-layer adsorption. The parameter K_F refers to the relative adsorption capacity, i.e., ZIF-8 exhibits higher TPE adsorption capacity at 283K than at 303K, according to the K_F data shown in Table S1. Based on equation (3), a straight line was obtained when plotting $\ln q_e$ vs. $\ln C_e$ (Fig.S6). The constants, K_F and n, are then defined by the intercepts and slops of the line, respectively. It appears that the Freundlich model agrees well with obtained experimental data (Table S1), with the correlation coefficient values being close to 1 at different temperatures. The TPE adsorption capacity decreases with the rise of temperatures, indicating an exothermic reaction. Thermodynamic parameters can be calculated from the variation of the thermodynamic equilibrium constant K_0 with the change in temperature. For adsorption reactions, K_0 is defined as follows:

$$K_0 = \frac{C_s}{C_e} \quad (4)$$

Where K_0 is the adsorption equilibrium constant, C_s the amount of TPE adsorbed per mass of ZIF-8 (mg g^{-1}), C_e the TPE concentration in solution at equilibrium (mg L^{-1}). As the TPE concentration in the solution decreases and approaches zero, K_0 can be obtained by plotting $\ln(C_s/C_e)$ vs. C_s (Fig.S7) and extrapolating C_e to zero. The adsorption standard free energy changes (ΔG^0) can be calculated according to the equation (5):

$$\Delta G^0 = -RT \ln K_0 \quad (5)$$

$$\ln K_0(T_2) - \ln K_0(T_1) = \frac{-\Delta H^0}{R}\left(\frac{1}{T_2} - \frac{1}{T_1}\right) \quad (6)$$

$$\Delta S^0 = -\frac{\Delta G^0 - \Delta H^0}{T} \quad (7)$$

Where R universal gas constant (1.987 cal deg^{-1} mol^{-1}), and T is the temperature in Kelvin. The average standard enthalpy change (ΔH^0) is obtained from Van't Hoff equation (6). Where, T_3 and T_1 are two different temperatures. The standard entropy change (ΔS^0) can be obtained by the equation (7) [42].

The thermodynamic parameters are list in Table 2. A negative standard enthalpy change suggests that the interaction of TPE adsorbed by ZIF-8 is exothermic, which is supported by the decreasing adsorption of TPE with the increase in temperature. A negative ΔG^0 indicate that the adsorption reaction is a spontaneous process. The negative ΔS^0 is unfavourable for spontaneous adsorption of TPE on ZIF-8. However, the negative ΔH^0 is favourable for spontaneous adsorption of TPE on ZIF-8. Therefore, the driving force for the adsorption of TPE on ZIF-8 is controlled by an enthalpy change rather than an entropy effect.

Table 2 Thermodynamic parameters for adsorption of TPE on ZIF-8

Temperature(K)	Thermodynamic constant		
	$\triangle G^0$	$\triangle H^0$	$\triangle S^0$
283.15	-1.084	-12.028	-0.039
293.15	-0.855	-12.028	-0.038
303.15	-0.311	-12.028	-0.039

Insights in preliminary mechanism for the selective adsorption of TPE on ZIF-8

Molecular-sieving effect In the present work, a similar result for selective and efficient adsorption of TPE over its substituted isomers including of CFE and DPE with only an alteration of 4-N of xanthine moiety was obtained through both sole adsorption and mixed adsorption experiments. As shown in Fig.S1, molecular sizes of TPE and CFE, DPE are larger than 3.4 Å of pore aperture diameter of nanoscale ZIF-8. The sole imidazole moiety of TPE is smaller than 3.4 Å. In careful comparison to TPE, CFE and DPE with larger molecular size and hydroxylpropoxyl branched configuration was further hindered to be adsorbed on ZIF-8 similar to the previous report for the ZIF-8 based molecular sieving of branched alkanes from linear alkanes.[25,43,44] Part embedding process was possibly occurred for the guest molecules described above adsorption on ZIF-8 as shown in Fig.S8. Besides, slighter adsorption capacity of CFE on ZIF-8 with an enhancement of hydrophobic effect by one methyl-substituted at 4-N of xanthine skeleton comparison to TPE demonstrated that only an alteration of substituent will give a synergic effect on the multiple interactions between the target and the adsorbent. N_2 adsorption–desorption experiment of ZIF-8 which adsorbed the TPE was performed to further study the molecular-sieving effect. The N_2 sorption experiment data which compared with sole ZIF-8 are added in supporting information (Fig.S9 and Table S2). The composites (ZIF-8 which adsorbed the TPE) was attributed to type I isotherms, with steep increases in N_2 uptake at a low relative pressure (<0.01), as does ZIF-8, which indicated the characteristics of microporosity. In comparison to the sole ZIF-8, the composites showed decreased Langmuir surface areas, the pore size, as well as pore volume as shown in Table S2 resulting from the molecular-sieving effect [45].

π–π interaction The π–π interaction between the aromatic conjugation rings of TPE and the aromatic imidazole rings of the ZIF-8 should be in consideration for efficient adsorption of TPE on ZIF-8. UV-vis spectra were used to study the π–π interaction between TPE and ZIF-8. Upon addition of the as-prepared ZIF-8 or 2-methylimidazole resulted to an obvious increase in the absorption band shorter than 255 nm for the TPE, simultaneous with a slight bathochromic shift of the main absorption peak from 271 nm to 273 nm as shown in Fig.4. The bathochromic shift of the main absorption band implied π–π interaction between TPE and ZIF-8.[46]The above results suggested that the π–π interaction played a crucial role for the efficient adsorption of TPE on ZIF-8.

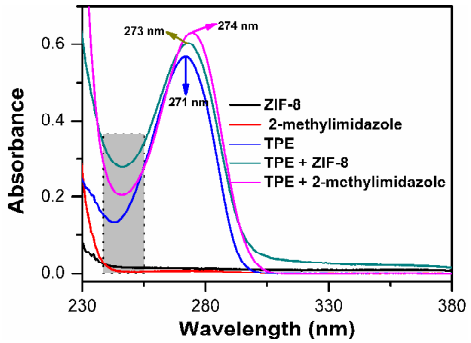

Fig.4 UV absorption spectra of TPE with ZIF-8 and 2-methlyimidazole in aqueous solution.

Zn-O coordination Inspired by small guest molecules adsorption on ZIF through a great variety of acido-basic sites (in particular low-coordinated Zn atoms) located at the external surface of ZIF-8 probed by FTIR and *ab* Initio calculations,[47] Zn-O coordination is also responsible for the efficient adsorption of TPE on ZIF-8 except for molecular-sieving effect and π–π interactions described as above. To validate this hypothesis, FT-IR spectrum was firstly used to probe the potential Zn-O coordination which is the interaction of O atom assigned to carbonyl group of TPE molecule with the transition metal ions on the ZIF-8 as shown in Fig.5a and b. It is worthy to note that no signal appearance for ZIF-8 only in the region 1900-1600 cm^{-1} was favoured of extraction of a set of important information. The two characteristic absorption bands at 1713 cm^{-1} and 1667 cm^{-1} assigned to vibration of carbonyl groups of TPE blue-shifted to 1698 cm^{-1} and 1651 cm^{-1} respectively after adsorption on ZIF-8 which was attributed to the interaction the carbonyl groups and unsaturated Zn species in ZIF-8. A similar result for the negative shift of the two bands to 1697 cm^{-1} and 1650 cm^{-1} obtained by directly mixed TPE with Zn^{2+} ions further identified the coordination interaction of open Zn species and carbonyl groups of TPE.[48-50] However, no significant change was observed for CFE and DPE due to either poor interaction between guest molecules or negligible adsorption capacity (Fig.S10). For better understanding of the Zn-O coordination effect, XPS experiments were carried out on ZIF-8 and TPE before and after adsorption depicted in Fig.5c and d. The XPS spectra showed that adsorption of TPE on ZIF-8 led to a shift to higher energy for O1s peak of the TPE (from 530.02 eV to 530.82 eV), as well as a shift of

lower energy for Zn 2p peak in ZIF-8 (from 1025.02 eV and 1044.47 eV to 1024.07 eV and 1044.12 eV, respectively). Although the open metal site in ZIF-8 have been occupied by water molecules though the coordination in aqueous solution, the adsorbed water molecules can still be replaced by other stronger affinity species. A pilot study was performed to try to identify the potential coordination effect between ZIF-8 and the adsorbed guest molecule. Except for the preliminary experiments (IR and XPS) above-mentioned, 8-hydroxyquinoline, a prototypical transition metal ions coordination agent, was chosen to probe the low-coordinated Zn species in ZIF-8. As shown in Fig.S11, no obvious change for XRD patterns of ZIF-8 and after adsorption of 8-HQ indicated that crystal structure of nanoscale ZIF-8 kept stable after adsorption of 8-HQ on ZIF-8. It needed to note that the maximum absorption wavelength of 8-hydroxyquinoline showed a significant bathochromic shift after the adsorption of 8-hydroxyquinoline on ZIF-8 as same as direct mixing of 8-hydroxyquinoline and zinc nitrate hexahydrate. To further identify the coordination interaction of Zn species in ZIF-8 with 8-HQ not the free Zn species in the filtrate, no bathochromic shift was observed for the filtrate of ZIF-8 was mixed with 8-hydroxyquinoline as shown in Fig.S12

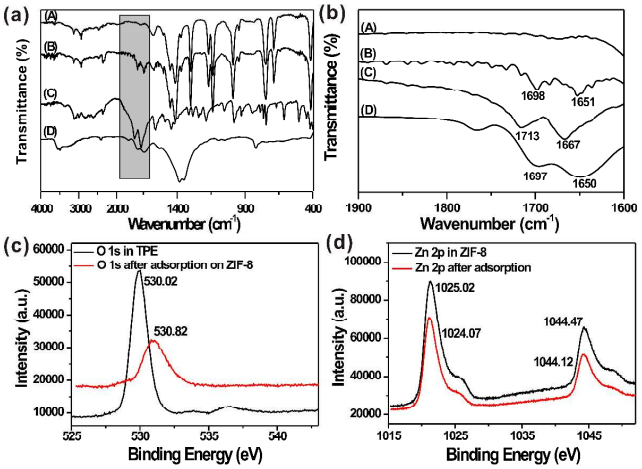

Fig.5 The full scan (a) and the amplified FT-IR spectra (b) for sole ZIF-8 (curve A), ZIF-8 after adsorbing TPE (curve B), TPE only (curve C) and TPE coordination with Zn^{2+} ions (curve D); XPS spectra of (c) O 1s in pure TPE and after adsorption on ZIF-8 and (d) Zn 2p in ZIF-8 and after adsorption of TPE on surface of ZIF-8.

Desorption and reusability of ZIF-8

Facile desorption of the target from adsorbents is very important for the collection of both the target and adsorbents in view of environmental-friendly and practical application. For this purpose,

acetonitrile alone, pH=11.0 Tris solution, 0.1% ammonia and 0.1 M NaOH aqueous solutions were tested to desorb TPE, CFE and DPE from nanoscale ZIF-8 (Table S3). The results show that 0.1 M NaOH gave the most efficient desorption capacity of three pharmaceutical analogs from preadsorbed ZIF-8 nanocrystals in aqueous solution. To further study the reusability of ZIF-8, adsorption experiment between the mixture solution and ZIF-8 was performed. For each run, the spent ZIF-8 adsorbed the mixture of TPE, CFE and DPE and then was eluted by solvent (pH=11.0 Tris solution). The eluted ZIF-8 was used for the next adsorption cycle after dried in 100˚C. Table S4 showed the good reusability and selectivity adsorption capacity of ZIF-8 after used for 5 times.

Solid phase extraction with the ZIF-8 as sorbent

Furthermore, a pilot study in a pseudo-solid phase extraction of drugs was performed to verify the feasibility of ZIF-8 as a novel on-line SPE sorbent for potential application in pharmacokinetics.

Table 3 SPE recovery of TPE, CFE and DPE in complex matrixes

Sample	TPE (%)	CFE (%)	DPE (%)
Plasma	26.70	0.00	0.00
Precipitated-plasma	77.90	5.90	3.90
Milk	54.80	33.90	34.70

As shown in Table 3, a considerable recovery change from 26.70% to 77.90% for TPE with a high selectivity for adsorption and desorption makes ZIF-8 a promising candidate sorbent.

Conclusion

In summary, we have demonstrated the adsorption of theophylline from aqueous solution on a highly porous zeolitic imidazolate framework-8 from the adsorption isotherm, kinetics, and desorption of the sorbent point of view. The highly selective and efficient adsorption of TPE on ZIF-8 over its structure-related analogs including of CFE and DPE take advantages of multiple interactions between the target and the adsorbent involving of molecular size and configuration effect, π–π interactions and low coordination metal species coordination effect. The high adsorption capacity, molecular-sieving effect, and exceptional chemical stability make ZIF-8 promising as a novel adsorbent for the adsorption and extraction of pharmaceuticals from complex matrix which is of great significance for applications in pharmacokinetics.

Acknowledgement

The authors gratefully acknowledge the financial support for this work from the National Natural Science Foundation of China (Grant Nos. 21305161 and 81202576), the Natural Science Foundation of Jiangsu Province (Grant No. BK20130643).

References

1. M. Kawai, M. Kato, *Methods Find. Exp. Clin. Pharmacol.,* 2000, **22**, 309.
2. D. J. Rowe, I. D. Watson, J. Williams, D. J. Berry, *Ann. Clin. Biochem.,* 1988, **25**, 4.
3. G. Herrmann, M. B. Aynesworth, J. Martin, *J. Lab. Clin. Med.,* 1937, **23**, 135.
4. J. W. Daly, *J. Med. Chem.,* 1982, **25**, 197.
5. K. M. Piafsky and R. I. Ogiivie, *N. Engl. J. Med.,* 1975, **292**, 1218.
6. R. C. Gupta, G. D. Lundberg, *Anal. Chem.,* 1973, **45**, 2403.
7. M. Homma, K. Oka, N. Takahashi, *Anal. Chem.,* 1989, ***61***, 784.
8. E. P. Lai, E. Dabek - Zlotorzynska, *Electrophoresis,* 1999, ***20***, 2366.
9. W. M. Mullett, E. P. C.Lai, *Anal. Chem.,* 1998, **70**, 3636.
10. J. Niu, Z. Liu, L. Fu, F. Shi, H. Ma, Y. Ozaki, X. Zhang, *Langmuir*, 2008, **24**, 11988.
11. Y. Sueyoshi, C. Fukushima, M. Yoshikawa, *J. Membr. Sci.,* 2010, **357**, 90.
12. C. Wang, Z.Q. Shi, R.F. Wang, *Chem. J. Chin.Univ.,* 2003, **24**, 1896.
13. H. Furukawa, K. E. Cordova, M. O'Keeffe, O. M. Yaghi, *Science*,2013, **341**, 1230444.

14. Z.-Y. Gu, Y.-J. Chen, J.-Q. Jiang, X.-P. Yan, *Chem. Commun*., 2011, **47**, 4787.
15. N. A. Khan, Z. Hasan, S. H. Jhung, *J. Hazard. Mater.,* 2013, **244–245**, 444-456.
16. N. A. Khan, Z. Hasan, S. H. Jhung, *J. Hazard. Mater.,* 2013, 24416.
17. K. S. Park, Z. Ni, A. P. Côté, J. Y. Choi, R. Huang, F. J. Uribe-Romo, H. K. Chae, M. O'Keeffe, O. M. Yaghi, *PNAS.,* 2006, **103**, 10186.
18. R. Banerjee, A. Phan, B. Wang, C. Knobler, H. Furukawa, M. O'Keeffe, O. M. Yaghi, *Science,* 2008, **319**, 939.
19. J. C. Tan, T. D. Bennett, A. K. Cheetham, *PNAS.,* 2010, 107, 9938.
20. G. Lu, S. Li, Z. Guo, O. K. Farha, B. G. Hauser, X. Qi, Y. Wang, X. Wang, S. Han, X. Liu, J. S. DuChene, H. Zhang, Q. Zhang, X. Chen, J. Ma, S. C. J. Loo, W. D. Wei, Y. Yang, J. T. Hupp, F. Huo, *Nat. Chem.,* 2012, **4**, 310.
21. D. Ge, H. K. Lee, *J. Chromatogr. A,* 2011, **1218**, 8490.
22. D. Ge, H. K. Lee, *J. Chromatogr. A,* 2012, **1263**, 1.
23. D. Ge, H. K. Lee, *J. Chromatogr. A,* 2012, **1257**, 19.
24. X.-Q. Yang, C.-X. Yang, X.-P. Yan, *J. Chromatogr. A,* 2013, **1304**, 28.
25 K. Li, D. H. Olson, J. Seidel, T. J. Emge, H. Gong, H. Zeng, J. Li, *J. Am. Chem. Soc.,* 2009, **131**, 10368.
26. N. Chang, Z.-Y. Gu, X.-P. Yan, *J. Am. Chem. Soc.,* 2010, **132**, 13645.
27. G. Lu, J. T. Hupp, *J. Am. Chem. Soc.,* 2010, **132**, 7832.
28. L.-M. Li, H.-F. Wang and X.-P. Yan, *Electrophoresis,* 2012, **33**, 2896.
29. Y.-Y. Fu, C.-X. Yang and X.-P. Yan, *Chem.-Eur. J.*, 2013, **19**, 13484.
30. X.-Z. Kang, Z.-W. Song, Q. Shi and J.-X. Dong, *Asian J. Chem.*, 2013, **25**, 8324.
31. X. Liu, H. Jin, Y. Li, H. Bux, Z. Hu, Y. Ban and W. Yang, *J. Membr. Sci.*, 2013, **428**, 498.
32. Y.N. Wu, M. Zhou, B. Zhang, B. Wu, J. Li, J. Qiao, X. Guan, F. Li, *Nanoscale,* 2014, **6**, 1105-1112.
33. J.-Q. Jiang, C.-X. Yang and X.-P. Yan, ACS *Appl. Mater.* Interfaces, 2013, **5**, 9837.
34. K. A. Cychosz, A. J. Matzger, *Langmuir*, 2010, **26**, 17198.
35. G. Crini, H. N. Peindy, F. Gimbert and C. Robert, *Sep. Purif. Technol.,* 2007, **53**, 97.
36. S.Wang, H.Li, L.Xu, *J. Colloid Interface Sci.,* 2006, **295**, 71.
37. E. Haque, J. E. Lee, I. T. Jang, Y. K. Hwang, J.-S. Chang, J. Jegal, S. H. Jhung, *J. Hazard. Mater.* 2010, **181**, 535−542.
38. Huo, S.-H.; Yan, X.-P. J. *Mater. Chem.,* 2012, **22**, 7449−7455.
39. V. Vadivelan and K. V. Kumar, *J. Colloid Interface Sci.,* 2005, **286**, 90.
40. E. Bulut, M. Ozacar and I. A. Sengil, *Microporous Mesoporous Mater.,* 2008, **115**, 234.
41. L. Wang, J. Zhang, R. Zhao, C. Li, Y. Li and C. L. Zhang, *Desalination*, 2010, **254**, 68.
42. V. J. P. Poots, G. McKay and J. J. Healy, *J.-Water Pollut. Control Fed.,* 1978, **50**, 926.
43. C.-L. Hsueh, Y.-W. Lu, C.-C. Hung, Y.-H. Huang, C.-Y. Chen, Dyes and pigments 2007, **75**, 130.
44. N. Chang, Z.-Y. Gu, H.-F. Wang, X.-P. Yan, *Anal. Chem.,* 2011, **83**, 7094.
45. C. Zhang, R. P. Lively, K. Zhang, J. R. Johnson, O. Karvan, W. J. Koros, *J. Phys. Chem. Lett.,* 2012, **3**, 2130.
46. G. Lu, S. Z. Li, Z. Guo, et al. *Nat. Chem.*, 2012, **4**, 310.
47. B. Song, H. Wei, Z. Q.Wang, X. Zhang, M. Smet, W.Dehaen, *Adv. Mater.,* 2007, **19**, 416.
48. C. Chizallet, S. Lazare, D. Bazer-Bachi, F. Bonnier, V. Lecocq, E. Soyer, A.-A. Quoineaud, N. Bats, *J. Am. Chem. Soc.,* 2010, **132**, 12365.
49. L. G. Marzilli, T. J. Kistenmacher, C.-H. Chang, *J. Am. Chem. Soc.,* 1973, **95**, 7507.
50. C. O. Arean, A. A. Tsyganenko, E. E. Platero, E. Garrone, A. Zecchina, *Angew. Chem., Int. Ed.,* 1998, **37**, 3161.
51. E. Garrone, B. Fubini, B. Bonelli, B.Onida, C. Otero Arean, *Phys. Chem. Chem. Phys.,* 1999, **1**, 513.